論文 / 著書情報
Article / Book Information

Title	DESIGN METHOD FOR EXISTING TALL BUILDINGS USING OIL DAMPERS AND BRACES WITH DISPLACEMENT GAP
Authors	D. Sato, K. Watai, F. Ueno, K. Kasai, K. Saburi, T. Maeda, H. Masuda
Pub. date	2020, 9
Citation	2020 17WCEE Proceedings

17th World Conference on Earthquake Engineering, 17WCEE
Sendai, Japan - September 13th to 18th 2020

DESIGN METHOD FOR EXISTING TALL BUILDINGS USING OIL DAMPERS AND BRACES WITH DISPLACEMENT GAP

D. Sato[1], K. Watai[2], F. Ueno[3], K. Kasai[4], K. Saburi[5], T Maeda[6] and H. Masuda [7]

[1] *Associate Professor, Tokyo Institute of Technology, sato.d.aa@m.titech.ac.jp*
[2] *Specially Appointed Assist. Prof., Tokyo Institute of Technology, watai.k.aa@m.titech.ac.jp*
[3] *Graduate student, Tokyo Institute of Technology, ueno.f.aa@m.titech.ac.jp*
[4] *Specially. Prof., Tokyo Institute of Technology, kasai.k.ac@m.titech.ac.jp*
[5] *Takenaka Corporation, saburi.kazuhiro@takenaka.co.jp*
[6] *Takenaka Corporation, maeda.tatsuhiko@takenaka.co.jp*
[7] *Takenaka Corporation, masuda.hiroyukia@takenaka.co.jp*

Abstract

In the near future, substantial long-period ground motion (e.g., Nankai Trough) is expected to occur in Japan. These long-period ground motions may be stronger than existing design ground motions. Hence, considerable major damage to existing tall buildings is anticipated. To mitigate this damage, several retrofits that install dampers in existing buildings are being studied. However, existing buildings have limited places where such dampers can be installed. Therefore, a design method that considers the existing restrictions is necessary. It is also desirable to have a fail-safe mechanism that suppresses excessive deformation in anticipation of more ground motion than expected. Therefore, for existing tall buildings, we propose a design method that uses oil dampers and braces with displacement gaps (gap-brace). In this method, the response is controlled only by oil dampers for normal earthquake motion, and the deformation is controlled by the action of gap-braces with hardening characteristics for a strong earthquake. In addition, the proposed method can consider the limitations regarding the damper location and can set the gap and brace stiffness appropriately for suppressing the increase in shear force. To validate this method, a 37-story steel structure building model comprising members, and two types of ground motion—having long and short periods—were used. First, a time history response analysis was performed using an analysis model in which only oil dampers were installed considering the location of the damper. Consequently, the deformation of the building was generally within the target however, the upper story of building was larger than the target deformation owing to the influence of higher-order modes. Therefore, a brace with a gap was installed only in the story exceeding the target deformation. Second, a time history response analysis was performed using an analysis model with oil dampers and gap-braces designed using this method. From the results, it was confirmed that the deformation can be controlled and that the increase in the shear force can be suppressed even for a strong earthquake.

Keywords: Existing tall building; Seismic retrofit; Oil damper; Braces with gap

1. Introduction

In the near future, long-period ground motions due to the Nankai Trough Earthquake are expected to occur in three major metropolitan areas in Japan (e.g., Kanto, Chukyo, Osaka). Thus, there are a concern regarding tall buildings being damaged. As a countermeasure, in 2016, the Ministry of Land, Infrastructure and Transport provided technical advice and formulated long-period ground motions for design of tall buildings [1]. Long-period ground motions are larger than previous seismic waves used in designs. Therefore, the seismic resistance of existing tall buildings to such ground motions should be verified. As a result, some buildings may need renovation. As methods of renovating for those existing buildings, seismic resistance, seismic isolation, and vibration control retrofit can be considered. A period of the building is shortened when seismic retrofitting methods are used, which may increase the input energy to the building. In contrast, when seismic isolation retrofitting is adopted, the period of the building becomes longer and is affected by long-period ground motion. Furthermore, it is not easy because the retrofitting of the seismic isolation story is large. Therefore, to prepare for large-amplitude earthquake motion without changing the natural period of the tall building, the retrofit using vibration dampers is considered [2 - 4]. However, in the case of existing buildings, it is difficult to design a damper that satisfies the criteria because there are more restrictions, such as the difficulty in changing the architectural plan and the strength of peripheral members, compared to new constructed buildings. Therefore, there is a need for a mechanism that exhibits a high deformation control effect even in situations where the installation position is limited.

For the passively controlled design of buildings using oil dampers, Kasai and Nishimura [5] proposed a method of arranging oil dampers in proportion to the building stiffness; this method was adopted in another study [6]. Afterward, Kasai and Ito [7] proposed a design method that uses the equivalent rigidity adjustment method considering the rigidity distribution of the building. However, these design methods involve a high degree of freedom with respect to the damper installation position, assuming a new construction. In contrast, there have been several studies on damping systems that combine dampers and deformation control mechanisms that functions as a fail-safe only in the case of large-amplitude ground motion. Kawamata and Sato et al. [8] proposed a system that involves installing a vibration damper and a deformation control mechanism on the frame. It becomes a passively controlled structure for small deformations and a brace structure owing to the deformation control mechanism for large deformations. From the results of static loading experiments and shaking table excitation tests on a three-story frame equipped with this mechanism, it was confirmed that the maximum inter-story deformation angle was reduced and uniformized through the deformation control mechanism [8]. Nomura and Sato et al. [9] used an 8-story member structure model. Hayashi and Minami et al. [10] showed that applying the deformation control mechanism to a 50-story shear model and using it together with a viscous damper resulted in substantial reductions in the inter-story deformation angle. The authors of another study [11] applied the deformation control mechanism to a 37-story member structure model, and analyzed the model using its stiffness and the gap as parameters. From the results, it was confirmed that the rigidity of the deformation control mechanism decreased, and the gap increased owing to the effect of the deformation of the surrounding frame and the deformation control mechanism of other stories. In particular, this phenomenon was observed in the upper floors of a high-rise building, and these effects should be considered when applying the deformation control mechanism to high-rise buildings. Inoue and Honma et al. [12] have proposed a simple method to calculate the required damper size and gap based on the energy method. This method ensures that the response plasticity of each story is lower than the target value. The method was validated using a shear model of an 11-story RC building. Nomura and Sato et al. [13] presented a response prediction and design method for a single-degree-of-freedom model with a deformation control mechanism based on the energy method.

The purpose of this study is to propose a seismic retrofit design method using oil dampers and deformation control mechanisms (gap brace), considering the constraints on existing tall buildings.

2. Response characteristics without dampers

2.1 Overview of analysis model

Fig. 1 shows an existing high-rise building (no-damper model) [14]. In this paper, the X-direction is the subject of study, and the oil dampers and gap braces have their installation restricted to the height direction of the X4 to X7 spans of the Y3 frame, as shown in Fig. 1. The natural periods in the X direction of the no-damper model are 4.82 s, 1.67 s, and 0.99 s for first, second, and third modes, respectively. Fig. 2 shows the relationship between the story shear force Qi and the story deformation angle Ri obtained from the static load increment analysis. The plots in the figure show the elastic limit of each story. The elastic limit is reached at approximately 1/150 rad. for all stories, and the standard shear force coefficient at the story deformation angle reaching the elastic limit C0 is 0.3 to 0.4.

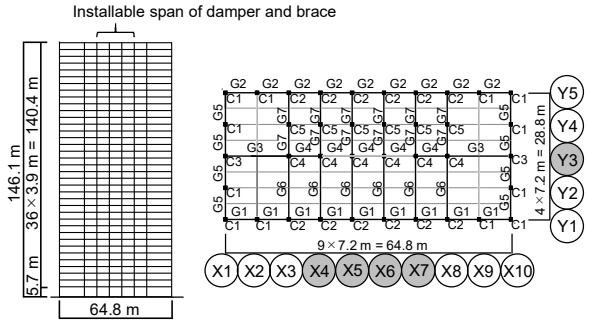

(a) Frame elevation（Y3）　(b) Typical floor plan

Fig.1 Overview of analysis model.

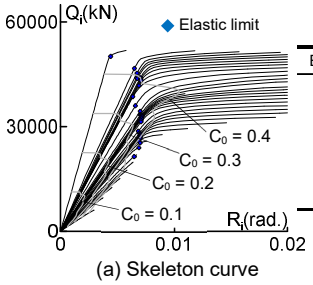

(a) Skeleton curve

Elastic limit story	13	Ulitimate state story	11
Q_{by} (kN)	37201	Q_{bu} (kN)	48474
C_{by}	0.072	C_{bu}	0.094
$C_{by}\cdot T_1$	0.348	$C_{bu}\cdot T_1$	0.468
δ_y (mm)	27.3	δ_u (mm)	78
R_y (rad.)	0.007	R_u (rad.)	0.02

(b) Detail of static analysis

Fig.2 Result of static analysis.

2.2 Outline of input earthquake

The long-period ground motion (OS2) in the Osaka region formulated by the Ministry of Land, Infrastructure, Transport and Tourism [1] and ART KOBE (Hyogoken-Nanbu Earthquake 1995 NS Phase: Level 2) were selected in this study. In addition, those seismic waves considering the amplification of the ground of the design site were used (OS2 & OS2-T and ART KOBE & ART KOBE-T). Figs. 3 (a) and 3 (b) show the acceleration time history of OS2 & OS2-T and ART KOBE &ART KOBE-T. Fig. 4 (a) to 4 (c) show the displacement, velocity and acceleration response spectra for those input earthquakes, respectively.

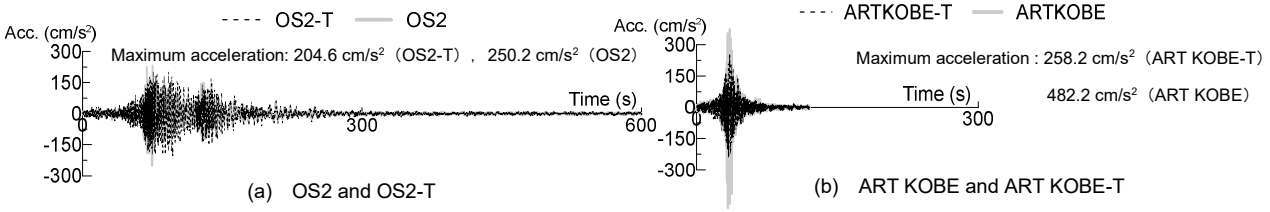

Fig.3 Acceleration time history.

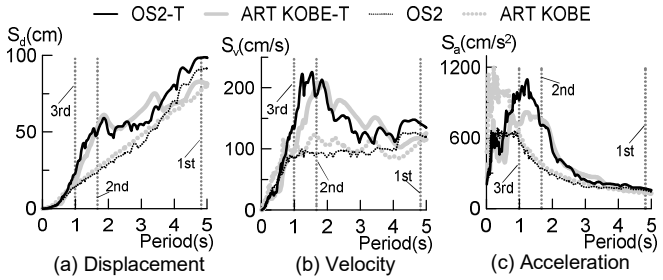

Fig.4 Response spectra (h = 0.05).

2.3 Earthquake response analysis (no-damper model)

OS2-T and ART KOBE-T were input to the no-damper model, and the response of each elasto-plastic analysis was examined. The structural damping constant was given in the initial-stiffness proportional damping, which is 2% of the first natural period, and the analysis step is Δt = 0.01 s. Fig. 5 (a) and (b) show the maximum story drift angle Ri and maximum acceleration A_i when OS2-T and ART KOBE-T are input, respectively. Although the response spectra of OS2-T and ART KOBE-T (Fig. 4) are similar, the largest R_i occurs in different stories when OS2-T and ART KOBE-T are input (Fig. 5 (a)). The maximum value of R_i exceeded 0.01 rad. It was expected that the main frame was plasticized. The largest A_i was over 400 cm/s^2 in the upper story (Fig. 5(b)).

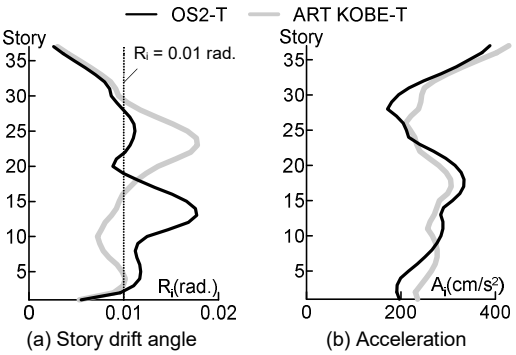

Fig.5 Maximum response (No-damper).

3. Seismic retrofit using oil dampers

3.1 Dynamic characteristics of SDOF model with oil damper

Fig. 6(a)-(c) show the force-deformation relationship of the viscous element, additional system, and system, respectively. The value obtained dividing the force at zero deformation (open circle) by the maximum deformation is defined as loss stiffness K''_d. Similarly, the value obtained dividing the force (black circle) at the maximum deformation by the maximum deformation is defined as the storage stiffness K'_d. A series combination of a viscous element and a support material having elastic stiffness K_b is called an additional system, and its force and deformation are F_a and u_a, respectively. Furthermore, the series connection of the elastic spring element of the damper and the support is defined as an equivalent support, and its rigidity is defined as K^*_b. In addition, the support material deformation ratio λ, which indicates the energy absorption efficiency of the viscous element in the additional system, is defined as follows:

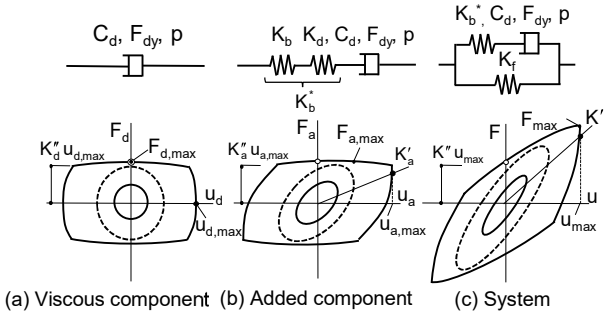

Fig.6 Relationship of load and displacement (oil damper).

$$\lambda = \frac{K''_d}{K^*_b} \tag{1}$$

The above equation shows that when the value of λ is large, the deformation of the support material is large, and the energy absorption efficiency of the damper is low. Furthermore, K''_d and K^*_b can be expressed by the following equations:

$$K''_d = C_d\,\omega \quad , \quad K^*_b = \frac{K_d \cdot K_b}{K_d + K_b} = \frac{(\beta/\omega)K''_d K_b}{(\beta/\omega)K''_d + K_b} \tag{2a,b}$$

where C_d is the viscosity coefficient; ω is the natural circular frequency of the building model; and β is the internal stiffness ratio. The storage and loss stiffness of the additional system can be expressed using the following equations:

$$K'_a = \frac{\lambda}{1+\lambda^2}K''_d \ , \ K''_a = \frac{1}{1+\lambda^2}K''_d \tag{3a,b}$$

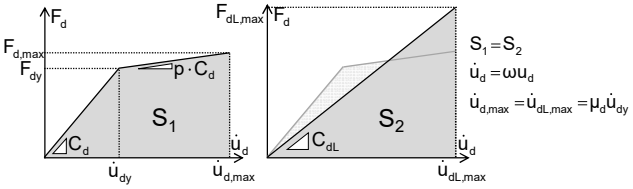

Fig.7 Equivalent linearization of oil damper

Fig. 7 shows the force F_d -velocity $\dot{u}_d$, relationship of the oil damper with the relief system and the force-velocity relationship after equivalent linearization. When the damper force F_d exceeds the relief load F_{dy}, C_d becomes pC_d. The velocity at this time is called the relief velocity $\dot{u}_{dy}(=F_{dy}/C_d)$, where p is the secondary viscosity ratio. The maximum amplitude $u_{d,\,max}$ divided by the amplitude at the time of the relief force $u_{dy}(=\dot{u}_{dy}/\omega)$ is defined as the relief rate μ_d [15]. If the bilinear viscous element is replaced with an equivalent linear viscous element related to the area enclosed by the skeletal curve shown in Fig. 7, Kasai et al [15] show that the maximum deformation and the maximum velocity of viscous element deformation for each system become almost the same against the earthquake input. The relationship between the linear element viscosity coefficient C_{dL} equivalent to the bilinear element C_d, μ_d, p at that time can be obtained from the following equation (S1 = S2, where, S1: the area in the bilinear state, S2: the area after linearization):

$$\frac{1}{2}(\dot{u}_{d,\max}F_{dy}+\dot{u}_{d,\max}F_{d,\max}-\dot{u}_{dy}F_{d,\max})=\frac{1}{2}u_{dL,\max}F_{dL,\max} \tag{4}$$

Hereafter, the equivalent linear value is represented by the subscript "L". By transforming Eq. (4), the following equation is obtained:

$$\frac{C_{dL}}{C_d}=p+\frac{2(1-p)}{\mu_d}-\frac{1-p}{\mu_d^2}=f(p,\mu_d)\cong\frac{K''_{dL}}{K''_d} \tag{5}$$

Based on Eq. (5), the equivalent support deformation ratio λ_L, the equivalent storage stiffness ratio and the equivalent loss stiffness ratio of the added component (K'_{aL}/K_f and K''_{aL}/K_f) are expressed by the following equations, respectively:

$$\lambda_L=\frac{K''_{dL}}{K_b^*}=\lambda\cdot f(p,\,\mu_d)\ ,\quad \frac{K'_{aL}}{K_f}=\frac{\lambda_L}{1+\lambda_L^2}\frac{K''_d}{K_f}\cdot f(p,\mu_d)\ ,\quad \frac{K''_{aL}}{K_f}=\frac{1}{1+\lambda_L^2}\frac{K''_d}{K_f}\cdot f(p,\mu_d) \tag{6, 7a,b}$$

The equivalent damping ratio of the system ζ_{eq} is obtained from the following equation:

$$\zeta_{eq}=\zeta_0+0.8\,\zeta'_{eq} \tag{8}$$

where ζ_0 is the structural damping ratio. ζ'_{eq} is the additional damping ratio by the oil damper, and is expressed by the following equation [17], [18]:

$$\zeta'_{eq}=\frac{K''_{aL}/K_f}{2(1+K'_{aL}/K_f)} \tag{9}$$

where ζ'_{eq} is the theoretical value of the damping ratio under the steady state with a sine wave disturbance corresponding to the equivalent linear system period T_{eqL}; T_{eqL} is expressed using the following equation [17], [18]:

$$T_{eqL}=T_f\sqrt{\frac{1}{1+K'_{aL}/K_f}} \tag{10}$$

However, in a random disturbance, components other than T_{eqL} are included, and the actual equivalent damping constant is lower than the theoretical value. Then, 0.8 in Eq. (8) represents the reduction rate [18].

3.2 Design procedure for seismic retrofit using oil dampers

Design procedure for seismic retrofit using oil dampers is shown below.

STEP 1: Setting specifications for the target building.

STEP 2: Calculating story deformation angle (no-damper model).

STEP 3: Setting target story deformation angle.

STEP 4: Calculating the required damper size in SDOF model.

STEP 5: Distributing required damper size to MDOF model.

STEP 6: Determining damper specifications for each story.

This paper proposes an equation that distributes the damper from a single-mass system in STEP 5 to a multi-mass system. In addition, referring to the non-proportional distribution of story stiffness proposed in Ref. [7], the constraints regarding damper installation are considered (Section 3.4). Furthermore, the maximum story shear envelope obtained from OS2-T and ART KOBE-T (no damper model, Section 3.5) is used to account for the effects of higher modes (Section 2.4).

3.3 Calculation of demanded damper size for SDOF model

The loss stiffness ratio K''_d / K_f and the equivalent damping ratio ζ_{eq} of the SDOF damper model are calculated using the performance curve as in Ref. [6]. The inter-story deformation angle θ_f is obtained from the displacement response spectrum S_d. Then, the first mode shape is assumed to be a straight. The target inter-story deformation angle θ_{max} of the seismic retrofitted building is set to 1/100 rad. However, to decrease the response of the higher-order mode to the ART KOBE-T, the calculation of the equivalent damping ratio ζ_{eq} is performed with θ_{max} = 1/125 rad, so the demanded damper size is increased. In this study, we obtained μ_d = 2.0, p = 0.02, β = 4.5, ζ_0 = 0.02, and the displacement reduction rate $R_d = \theta_{max} / \theta_f = 0.52$, and we obtained $K''_d / K_f = 0.336$ from the performance curve (Fig. 8). In Fig. 8, R_a is the shear force reduction rate. Furthermore, ζ_{eq} = 0.103 is obtained by substituting Eq. (7a, b) into Eq. (9) and considering $K''_d / K_f = 0.336$.

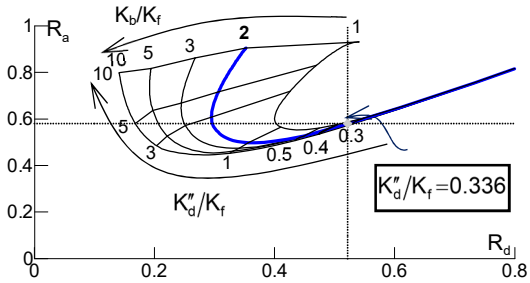

Fig.8 Performance curve.

3.3 Distribution method to MDOF model considering seismic retrofit restrictions

In this section, the method of distributing the K''_d / K_f of one SDOF model calculated in the previous section to MDOF model is proposed. Then, the constraint conditions are shown below.

a) The equivalent damping ratio of SDOF model and the MDOF model at θ_{max} are equal.

b) For the story where the damper is distributed non-proportionally, the story shear force obtained by multiplying the sum of the storage stiffness and the frame stiffness of each story at θ_{max} by the story deformation $h_i\theta_{max}$ is proportional to the system story shear force Q_i.

In addition, as the forces of the viscous element and the added component are always equal, the relationship between the amplitudes of the linear behavior is obtained as shown in the following equation [15]:

$$\frac{u_{d,\max}}{u_{a,\max}} = \frac{\dot{u}_{d,\max}}{\dot{u}_{a,\max}} = \frac{u_{dy}}{u_{ay}} = \frac{\dot{u}_{dy}}{\dot{u}_{ay}} = \frac{1}{\sqrt{1+\lambda^2}} \quad (\mu_d \le 1) \tag{11}$$

In this paper, with the restriction that the damper can be installed only in the height direction of the X4-X7 span of the Y3 frame, the following equation is obtained from the constraint a) and Eq. (11):

$$\frac{\pi K''_{dL} u^2_{L,\max} / (1+\lambda_L^2)}{2\pi (K'_{aL} + K_f) u^2_{L,\max}} = \frac{\pi \sum_A \{K''_{dL,\mathrm{op}} (h_i\theta_{\max})^2 / (1+\lambda_L^2)\} + \pi \sum_B \{K''_{dLi} (h_i\theta_{\max})^2 / (1+\lambda_L^2)\}}{2\pi \sum_A \{(K'_{aL,\mathrm{op}} + K_{fi})(h_i\theta_{\max})^2\} + 2\pi \sum_B \{(K'_{aLi} + K_{fi})(h_i\theta_{\max})^2\}} \tag{12}$$

Here, ΣA is the sum of the stories that specify arbitrary dampers, and ΣB: is the sum of the stories for which the dampers are calculated using the non-proportional distribution method of story stiffness; these items are followed by the subscript "op" when an arbitrary damper size is provided.

The following equation is obtained by solving Eq. (12) for $K''_{dL}/(K'_{aL} + K_f)$:

$$\frac{K''_{dL}}{K'_{aL}+K_f}=\frac{\sum_A(K''_{dL,\mathrm{op}}\,h_i^2)+\sum_B(K''_{dLi}\,h_i^2)}{\sum_A(K'_{aL,\mathrm{op}}+K_{fi})h_i^2+\sum_B(K'_{aLi}+K_{fi})h_i^2} \tag{13}$$

Here, from equation (3a), K'_{aL} and K'_{aLi} are obtained by the following equations:

$$K'_{aL}=\frac{\lambda_L}{1+\lambda_L^2}K''_{dL} \quad , \quad K'_{aLi}=\frac{\lambda_L}{1+\lambda_L^2}K''_{dLi} \tag{14}$$

Similarly, the following equation is derived from Eq. (3a):

$$K'_{aL,\mathrm{op}}=\frac{\lambda_L}{1+\lambda_L^2}K''_{dL,\mathrm{op}} \tag{15}$$

By substituting Eq. (14a) and Eq. (15) into Eq. (13), the following equation is obtained:

$$\frac{K''_{dL}}{K_f}=\frac{\sum_A(K''_{dL,\mathrm{op}}\,h_i^2)+\sum_B(K''_{dLi}\,h_i^2)}{\sum_{i=1}^{N}(K_{fi}h_i^2)} \tag{16}$$

In addition, from constraint b), the following equation is obtained:

$$\theta_{\max}=\frac{Q_i h_i}{(K'_{aLi}+K_{fi})h_i^2}=\frac{\sum_B Q_i h_i}{\sum_B(K'_{aLi}+K_{fi})h_i^2} \tag{17}$$

By substituting Eq. (15b) and (16) into Eq. (17) and solving for K''_{dLi}, the following equation is obtained:

$$K''_{dLi}=\frac{Q_i}{h_i}\left\{\frac{K''_{dL}}{K_f}\cdot\frac{\sum_{i=1}^{N}(K_{fi}h_i^2)}{\sum_B(Q_i h_i)}-\frac{\sum_A(K''_{dL,\mathrm{op}}h_i^2)}{\sum_B Q_i h_i}\right\}+\frac{1+\lambda_L^2}{\lambda_L}\cdot\frac{Q_i}{h_i}\cdot\frac{\sum_B(K_{fi}h_i^2)}{\sum_B Q_i h_i}-\frac{1+\lambda_L^2}{\lambda_L}\cdot K_{fi} \tag{18}$$

Finally, by substituting Eq. (6) into Eq. (18), K''_{di} can be obtained from the following equation considering the restriction on the damper installation position:

$$K''_{di}=\frac{Q_i}{h_i\sum_B Q_i h_i}\left\{\frac{K''_d}{K_f}\sum_{i=1}^{N}(K_{fi}h_i^2)-\sum_A(K''_{di,\mathrm{op}}\,h_i^2)+\Lambda\sum_B(K_{fi}h_i^2)\right\}-\Lambda K_{fi}\ ,\quad \Lambda=\lambda+\frac{1}{\lambda\{f(p,\,\mu_d)\}^2} \tag{19a, b}$$

In this design method, the calculations are repeated in the next step to obtain the final damper placement. However, the story that gives an optional damper size is $K''_{di} = K''_{di,op}$.

1) Using Eq. (19), calculate for all stories ($\Sigma_A = 0$). 2) If there is a story with $K''_{di} < 0$, give $K''_{di,op} = 0$ to the story and recalculate K''_{di} of the other story using Eq. (19). 3) If there is a story that exceeds the damper size that can be installed, $K''_{di,op} = K''_{di,\max}$ is given to the story for which the largest damper size is calculated, and K''_{di} of the other story is recalculated using Eq. (19). 4) Repeat 3) to obtain the final damper arrangement.

In this study, in step 1), $K''_{di} < 0$ in some lower and upper stories, and the negative damper size is calculated. This means that the frame stiffness K_{fi} of the corresponding story should be desirably reduced, as it is higher than necessary for the target maximum deformation angle $\theta_{\max}$. However, as previously mentioned, it is difficult to adjust the stiffness of the existing main frame for the seismic retrofit. In addition, if a negative damper size is calculated, an extremely large required damper size is calculated for other stories. This may not

be practical for the seismic retrofit of existing tall buildings. Here, in the method of Ref. [7], $\Sigma(K''_{di}\, h_i^2) / (K_{fi}\, h_i^2)$ and K''_d / K_f do not match because the K''_d of the story for which $K''_d < 0$ is calculated is set to 0 and the value is reduced to the upper limit at a constant rate for all stories. In contrast, in this proposed method, $K''_{di,op}$ is set for the story where $K''_{di} < 0$, and the maximum damper size $K''_{di,op} = K''_{di,\max}$ that can be installed is added to the story where K''_{di} is extremely large. By this method, it is possible to calculate K''_{di} for other stories so as to satisfy K''_d / K_f (Section 3.3) of SDOF model. In addition, $K''_d < 0$ in the lowermost story, but the calculation is performed with $K''_{di,op}$ given an arbitrary value assuming that a damper is installed without setting K''_{di}. That is, by using this method, the designer can add or reduce the dampers of the specific story according to the situation, and can recalculate the damper size of the other stories according to the arbitrary designated damper size. As a result, the value of K''_d / K_f in the MDOF model is the same as in the SDOF model.

3.5 Design example of seismic retrofit using oil dampers

Generally, an external force using an Ai distribution is used as a static external force for design, and the Ai distribution is also used in Ref. 7). However, as described in Chapter 2, in the case of tall buildings, it is necessary to consider the effects of higher-order modes, and the Ai distribution is not sufficient. Therefore, in this study, the damper design is performed using the envelope of the story shear force obtained from the elastic seismic response analysis of OS2-T and ART KOBE-T of the no-damper models (Envelope curve of Response Analysis, ERA). The dampers shown in Table 1 are used for the seismic retrofit in this study.

Table1 Specification of the using damper.

Damper name	1000kN	1500kN	2000kN
$\dot{u}_{dy}$(cm/s)	1.5		
C_d(kN · s/cm)	600	900	1200
p	0.0123		
β	4.5		
F_{dy}(kN)	900	1350	1800

Fig. 9 shows the initial calculated value and the value after redistribution of K''_{di}. Fig. 10 shows the frame stiffness ratio $K_{fi} / K_{fi,\max}$, the system story shear force ratio $Q_i / Q_{i,\max}$, and the damper size ratio $K''_{di} / K''_{di,\max}$ and their respective damper arrangements. Table 2 shows the specifications of each damper size (1000, 1500, and 2000 kN) arrangement. As shown in Fig. 9, when using the Ai distribution, a large value of K''_{di} is required near the 13th story. In contrast, when the ERA distribution is used, a large value of K''_{di} is required near the 13th and 23rd stories. In the case of the Ai distribution, the negative K''_{di} is calculated above the 29th story. In the case of the response ERA, the negative K''_{di} is calculated above the 32nd story. Therefore, $K''_{di} = 0$ is assigned to the aforementioned stories. As shown in Fig. 10, the non-proportional arrangement against the story stiffness distributes several dampers to a story having a large difference between the normalized story stiffness and the distribution of shear force. Therefore, it is confirmed that several dampers are arranged in the lower story in the case of Ai distribution and in the upper story in the case of ERA. Table 2 shows the equivalent damping ζ_{eq} of the MDOF model calculated using the modal strain energy method, assuming all interlaminar deformation angles to be uniform. In addition, the number of dampers N_d and the sum of the axial direction relief force of the dampers ΣF_{dy} are also shown in Table 2. From Table 2, it can be confirmed that each ζ_{eq} is reduced by approximately 10% compared with the equivalent damping constant of the SDOF model (ζ_{eq} = 0.103, section 3.3). This is

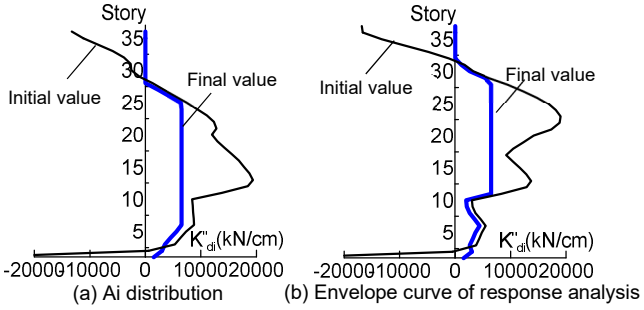

Fig.9 Calculation of damper values.

Table2 Specification of damper arrangements.

	Ai distribution	Envelope curve of response results
ζ_{eq}	0.084	0.086
ΣF_{dy}(kN)	262800	268200
N_d(Number)	148	160

because the damper specifications shown in Table 1 (1000, 1500, 2000 kN) were selected.

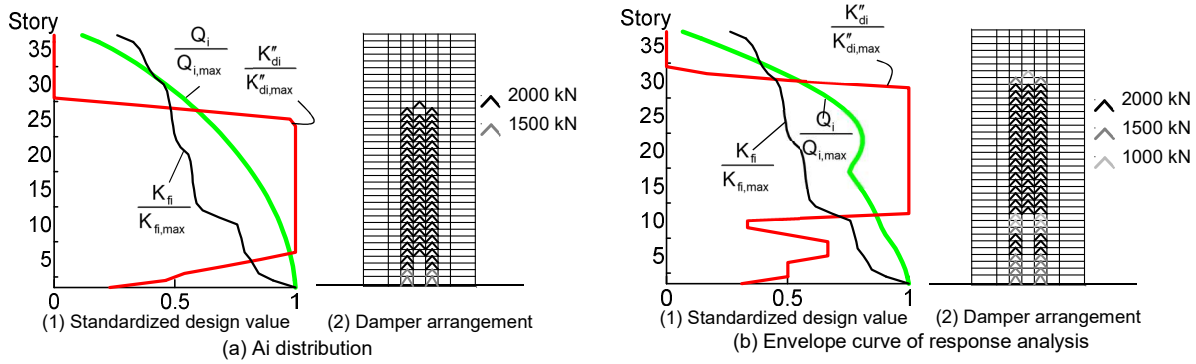

Fig.10 Overview of damper design.

3.6 Earthquake response analysis

Fig. 11 shows the maximum value distribution of the story deformation angle R_i, acceleration A_i and story shear force Q_i when OS2-T and ART KOBE-T are input to each model, respectively. In all models, R_i and A_i can be reduced by installing oil dampers compared to the no-damper model, and are almost within the target inter-story deformation angle R = 1/100 rad. However, even when ERA is used, it can be confirmed that the maximum inter-story deformation angle of 1/100 rad. or more occurs in stories 21 to 26 when ART KOBE-T is input.

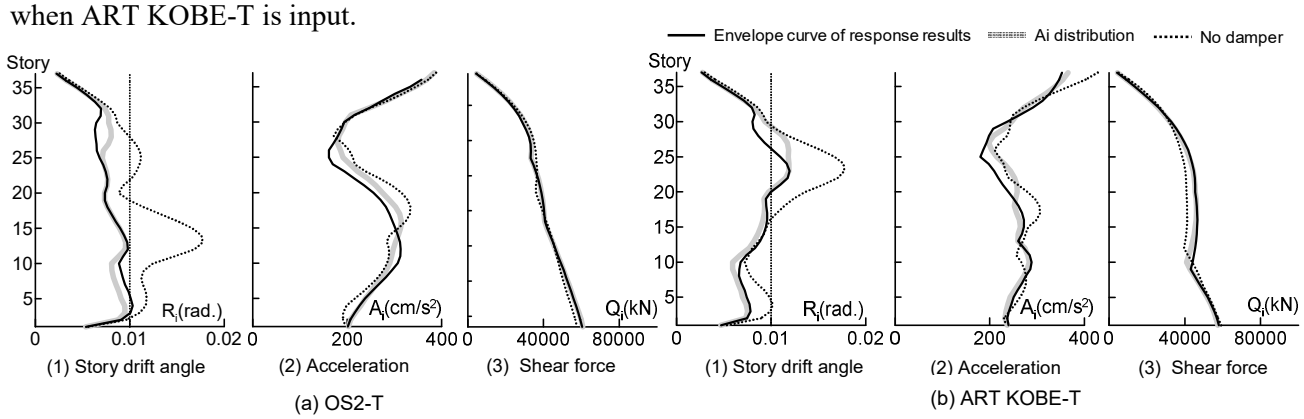

Fig.11 Maximum response (with oil dampers).

4. Seismic retrofit using oil damper and gap brace

As described in Chapter 3 (Model D), for some stories, the maximum story deformation angle of the installed oil dampers decided using ERA exceeded R = 1/100 rad. In this section, to solve this issue, we propose a new vibration control method that offers a higher degree of deformation control by replacing the oil dampers to gap braces.

4.1 Outline of Seismic retrofit using oil dampers and gap braces

Fig. 12 shows the force Q_i and story deformation Δu_i relationship of the member, additional system, and system of the gap brace, respectively. F_{gi} and F_{gai} in Fig. 12 are the horizontal forces in the member and additional system of the gap brace, respectively. In addition, u_{gai}, which is the sum of the gap brace horizontal deformation u_{ghi}, and the pseudo brace deformation of the member system, are equal to the

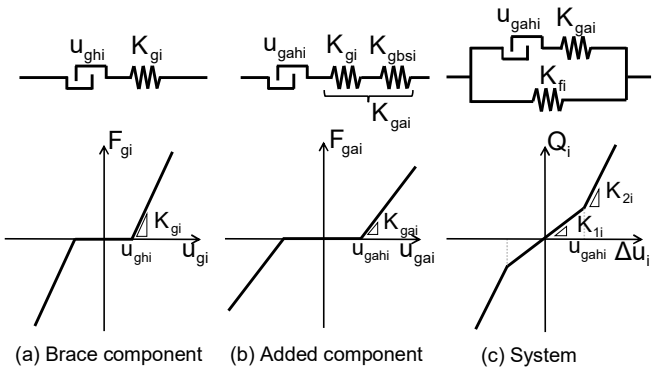

Fig.12 Relationship of load and displacement (gap brace).

story deformation Δu_i. Due to the effect of the deformation of the surrounding frame with the gap brace attached, the horizontal additional system stiffness K_{gai} is smaller than the horizontal stiffness of the gap brace K_{gi}. The pseudo brace stiffness K_{gbsi} is calculated using the state NR method, which converts a member configuration model to a horizontal spring system proposed by Kasai et al. [19, 20] (see section 4.3). Similarly, due to the deformation of the surrounding frame, the gap of the additional system u_{gahi} becomes larger than the gap of the member u_{ghi}. Fig. 13 shows a conceptual diagram of the gap brace design. In Fig. 13, K_{1i} is the frame stiffness (= K_{fi}) obtained from the static analysis, and K_{2i} is the system stiffness after the gap brace acts. In this paper, we designed the gap brace stiffness and gap to satisfy the target story deformation so that the maximum story shear force becomes equal before and after the gap brace is installed (from A to B in Fig 13).

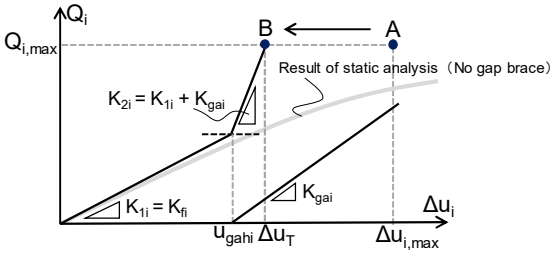

Fig.13 Conceptual diagram of gap brace design.

4.2 Procedures of seismic retrofit design

By setting the gap brace, the effect of controlling the deformation of the installation story is extremely high, but the deformation of the adjacent and other stories may increase. In addition, when installed in a multi-story structure, u_{gahi} is larger than u_{ghi}, so the deformation control effect intended in the design may not be obtained. Therefore, it is desirable to minimize the gap brace story placement. It is also desirable that the damping ratio of the system be the same before and after the installation of the gap brace. Procedures of seismic retrofit design using both oil dampers and gap braces are shown below.

Step 1. With the results of seismic response analysis of seismic retrofit using oil dampers (Section 3.6), we obtain $Q_i^D{}_{,\max}$ and $\Delta u_i^D{}_{,\max}$.

Step 2. The story where $\Delta u_T < \Delta u_i^D{}_{,\max}$ is decided as the gap brace installation story.

Step 3. Calculate K_{gbsi} for the spans where the gap braces are installed by the state NR method.

Step 4. Determine K_{gi} / K_{fi} and obtain the section of the gap brace A_{gi} from the following equation:

$$A_{gi} = \frac{K_{gi} L_{gi}}{E N_{gi} \cos^2 \theta_{gi}} \tag{20}$$

where, E is the Young's modulus, N_{gi} is the number of gap braces, θ_{gi} is the attached gap brace angle, and L_{gi} is the length of the gap braces.

Step 5. Using K_{gbsi} obtained in Step 3, K_{gai} is obtained from the following equation:

$$K_{gai} = \frac{K_{gi} \cdot K_{gbsi}}{K_{gi} + K_{gbsi}} \tag{21}$$

Step 6. Using K_{gai} obtained in Step 5, K_{2i} is obtained from the following equation:

$$K_{2i} = K_{1i} + K_{gai} = K_{fi} + K_{gai} \tag{22}$$

Step 7. The displacement u_{ghi} at the intersection of K_{1i} and K_{2i} passing through Δu_T and $Q_i^D{}_{,\max}$ is obtained in step 8.

Step 8. Using α_N, which is the ratio of the damper to the inter-story deformations in the state N, the gap of the member system u_{ghi} is obtained from the following equation:

$$u_{gahi} = \frac{K_{2i} \Delta u_t - Q_{i,\max}}{K_{1i} - K_{2i}} \tag{23}$$

where the gap brace with the smallest gap among the designed gap braces is applied to all the planned stories. If $u_{ghi} < 0$, return to Step 4 and increase K_{gi} / K_{fi}.

Step 9. Install a gap brace that satisfies A_{gi} and u_{ghi} obtained from Steps 4 and 8, respectively. If oil dampers are already installed, replace them with gap braces and redistribute the removed oil dampers according to section 3.4.

Fig. 13 (a) - (c) show the conceptual diagram of the state NR method, oil dampers and gap braces arrangement and the brace arrangement in the state NR method, respectively. Table 3 shows K_{gbsi} and α_N obtained from the state NR method.

4.3 Verification of seismic design method

Fig. 14 show the outline of the seismic retrofit model with oil dampers and gap braces designed according to the design procedure in section 4.2 (Model BD). Fig. 15(a) – (c) show the maximum story deformation angle R_i, acceleration A_i and story shear force Q_i, respectively, when ART KOBE-T is input to Model BD and Model D . Here, the results of two cases (K_{gi} / K_{fi} = 3.0 and 0.5) are shown in Fig. 15. From Fig. 15(a), it can be confirmed that the maximum story deformation angle R_i generally falls within the target story deformation angle (R = 1/100 rad). From Fig. 15(b) and (c), it can be confirmed that the proposed seismic retrofit design method using oil dampers and gap braces decreases the response story deformations and does not increase the response accelerations and story shear forces.

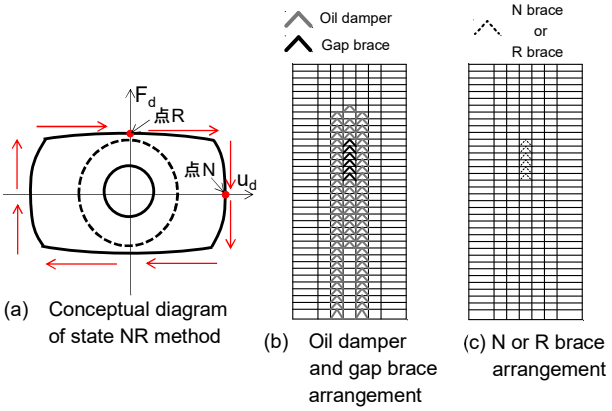

Fig.13 Overview of state NR method.

Table 3 List of K_{gbsi} and α_N.

層	K_{gbsi} [kN/cm]	K_{gbsi}/K_{fi} [－]	α_N [－]
26	2018	0.203	0.962
25	2097	0.209	0.964
24	2305	0.228	0.967
23	2702	0.265	0.969
22	3343	0.323	0.972
21	4181	0.389	0.972

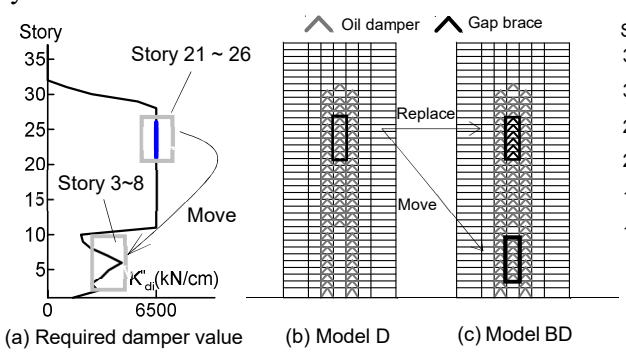

Fig.14 Overview of D and BD models.

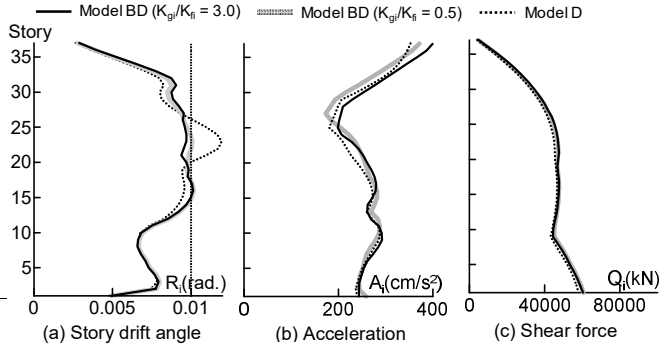

Fig.15 Maximum response (with oil damper and gap brace)
(Input ground motion : ART KOBE-T , Kgi/Kfi =0.5 3.0)

5. Conclusions

The purpose of this paper was to propose a seismic retrofit design method using oil dampers and gap braces considering the constraints on existing tall buildings. From the time history analysis results using the 37-story steel structure existing tall building model, it was confirmed that the proposed method decreases the response inter-story deformations and does not increase the response accelerations and story shear forces.

Acknowledgements
This work was supported by JST Program on Open Innovation Platform with Enterprises, Research Institute and Academia and TAKENAKA CORPORATION.

References

[1] Ministry of Land, Infrastructure, Transport and Tourism (2016): Countermeasures against long-period ground motion caused by a huge earthquake along the Nankai Trough in a high-rise building (Technical advice)
[2] Takuya Miyake et al. (2013): Design Method of Buildings Seismically Retrofitted by Eccentrically Connected Oil Dampers, *Summaries of Technical Papers of Annual Meeting*, pp.1225-1226
[3] Kazuhiro Fujishita et al. (2016): Optimization of Damper Arrangement with Hybrid GA using Elasto-Plastic Response Analysis on Seismic Response Control Retrofit, *Journal of Structural and Construction Engineering*, Vol.81, No.721, pp.537-546
[4] Kazuhiro Fujishita et al. (2018): Damper Arrangement with Hill-Climbing Method on Seismic Response Control Retrofit, *Summaries of Technical Papers of Annual Meeting*, pp.345-346
[5] Tadamune Nishimura et al. (2004): On Equivalent Linearization of Structure with Oil Dampers Part3: Design Method for MDOF, *Summaries of Technical Papers of Annual Meeting*, pp.65-66
[6] The Japan Society of Seismic isolation (2013); Manual for Design and Construction of Passively-Controlled Buildings
[7] Kazuhiko Kasai et al. (2008): Passive Control Design Method Based on Turning of Equivalent Stiffness of Bilinear Oil Damper, *Journal of Structural and Construction Engineering*, No.630, pp.1281-1288
[8] Daiki Sato at al. (2002): Vibration Response of a Passively Controlled Frame Having Nonlinear Restoring Force of Hardening Type, *The Japan Earthquake Engineering Symposium, proceedings*, Vol.11, pp.1649-1654
[9] Naoshi Nomura et al. (2013): Investigation of High Seismic Performance Structure Combining High Strength Steel with Damper and Deformation Control Mechanism by Member Structure Model, *Proceeding of the architectural research meetings*
[10] Hiroyuki Minami et al. (2012): Study on the Effect of Deformation–Control Systems against Pulse-Like Ground Motions, *AIJ Technol. Des*. Vol.18, No.39, pp.471-476
[11] Masuda Hiroyuki et al. (2019): Seismic retrofit considering extreme ground motion for existing super tall building Part 3: Seismic retrofit using oil dampers and gap braces, *Summaries of Technical Papers of Annual Meeting*, pp.865-866
[12] Makoto Honda et al. (2007): Energy Based Design of a System Combined of Damper and Displacement Controller for Seismically Excited Reinforced Concrete Structures, *Journal of Structural and Construction Engineering*, No.618, pp.49-56
[13] Naoshi Nomura et al. (2013): Energy Balance-Based Seismic Response Prediction Method of Flexible-Stiff Mixed Structure with Displacement Controller, *Journal of Structural and Construction Engineering*, No.692, pp.1705-1713
[14] Marina Nakagawa et al. (2013): Retrofit with Damper and Cumulative Damage Evaluation for Existing High-Rise Steel Building Subjected to Long-Period Ground Motion, *Summaries of Technical Papers of Annual Meeting*, pp.281-282
[15] Kazuhiko Kasai et al. (2004): Equivalent Linearization of Passive Control System with Oil Damper Bilinearly Dependent on Velocity, *Journal of Structural and Construction Engineering*, No.583, pp.47-54
[16] Kazuhiko Kasai et al. (2007): Equivalent between Linear and Bi-linear Viscous Elements Based on Passive Control Effectiveness, *Journal of Structural and Construction Engineering*, No.611, pp.29-37
[17] Kazuhiko Kasai et al. (2001): Kelvin-Type Formulation and Its Accuracy for Practical Modeling of Linear Viscoelastic Dampers Part 1 One-mass system having damper and elastic/inelastic frame, *Journal of Structural and Construction Engineering*, No.550, pp.71-78
[18] Kazuhiko Kasai et al. (2004): Evaluation Rule and Accuracy for Equivalent Period and Damping of Frequency-Dependent Passive Control Systems – Global damping model of one-mass system having elastic frame and either viscoelastic or oil damper –, *Journal of Structural and Construction Engineering*, No.580, pp.51-59
[19] Kazuhiko Kasai et al. (2006): Reduced Expression for Various Passive Control Systems and Conversion to Shear Spring Model, *Journal of Structural and Construction Engineering*, No.605, pp.37-46
[20] Masato Ishii et al. (2010): Shear Spring Model for Time History Analysis of Multi-Story Passive Controlled Buildings, *Journal of Structural and Construction Engineering*, Vol.75, No.647, pp.103-112

Note: All references are written in Japanese.

